Electronic Supplementary Material (ESI) for Dalton Transactions.
This journal is © The Royal Society of Chemistry 2021

Supporting Information

Luminescent Naphthalimide-Tagged Ruthenium(II)-Arene Complexes: Cellular Imaging, Photocytotoxicity and Transferrin Binding

Payal Srivastava, [a] *Madhu Verma,* [b] *Anmol Kumar,* [c] *Priyanka Srivastava,* [a] *Ramranjan Mishra,* [a] *Sri Sivakumar,* [b] *and Ashis K. Patra** [a]

[a] Department of Chemistry, Indian Institute of Technology Kanpur, Kanpur 208016, Uttar Pradesh, India.

[b] Department of Chemical Engineering and Centre for Environmental Science and Engineering, Indian Institute of Technology Kanpur, Kanpur 208016, Uttar Pradesh, India.

[c] School of Pharmacy, Computer-Aided Drug Design Center, University of Maryland, Baltimore, Maryland 21201, United States.

Table of Contents		Page
Stability Studies		3
Molecular Modeling		3
Scheme S1	Synthetic scheme for the preparation of the ligand L.	4
Figure S1	ESI-MS of the complex [**RuLCl**]	4
Figure S2	ESI-MS of the complex [**RuLPTA**]	5
Figure S3	FTIR spectra of complex [**RuLCl**] and [**RuLPTA**] in KBr phase.	5
Figure S4	^{1}H NMR spectra of [**RuLCl**] in DMSO-d_6	6
Figure S5	^{1}H NMR spectra of [**RuLPTA**] in DMSO-d_6	6
Table S1	Selected crystallographic table of complex [**RuLCl**]	7
Table S2	Selected bond lengths and angles of the complex [**RuLCl**]	8
Figure S6	^{1}H NMR spectra showing the stability of [**RuLCl**]	10
Figure S7	^{1}H NMR spectra showing the stability of [**RuLPTA**]	10
Figure S8	Time-dependent UV-visible spectral changes of complexes [**RuLCl**] and [**RuLPTA**]	11
Figure S9	Five sites used for molecular docking shown on the vdW surface of 2HAV and 3QYT	12
Figure S10	Conformation of [**RuLCl**] docked into the site1 and site2 on 2HAV	12
Figure S11	Conformation of [**RuLCl**] docked into the site1 and site2 on 3QYT	13
Table S3	Binding affinity of [**RuLCl**] at five different sites on 2HAV and 3QYT	13
Table S4	Binding affinity of [**RuLPTA**] at five different sites on 2HAV and 3QYT	14
Figure S12	MTT assay of the compounds in MCF-7 cancer cells	14
Figure S13	MTT assay of the compounds in A498 cancer cells	15
Figure S14	MTT assay of the compounds in HeLa cancer cells	15
Figure S15	MTT assay of the compounds in NRK normal cells	16
Figure S16	MTT assay of the compounds in NIH normal cells	16

Stability Studies

The stability of [**RuLCl**] and [**RuLPTA**] was determined by ^{1}H NMR spectroscopy in DMSO-d_6 after 24 h. No additional peaks were observed during the time period (Figure S6, S7). Integration of the peaks for both the complexes in DMSO-d_6 remain consistent with the reported spectra, suggesting higher stability in the solvent. However, the two chlorides attached to the Ru(II) ion in [**RuLCl**] can potentially undergo hydrolysis in an aqueous medium. To monitor anticipated hydrolysis, we monitored the time-dependent UV-vis spectral changes of the complexes at 298 K in a 4 mM NaCl-aqueous medium. The spectra displayed a decrease in the band centered at 360 nm, while an increase in the band at 440 nm (Figure S8a). However, when the experiment was carried out in 100 mM NaCl aqueous medium, no apparent spectral changes were observed and was found to be stable in such condition (Figure S8b). These data suggests that the complex possibly could remain stable in the bloodstream i.e., in high [Cl^-] (~100 mM) and will plausibly get aquated when it passes into the cell with low [Cl^-] (~4 mM). However, [**RuLPTA**] complex didn't show any noticeable spectral changes of the band at 440 nm in the 4 mM or 100 mM NaCl aqueous solution, while showed some changes in lower wavelength bands ~280 nm (Figure S4c and S4d). This may be due to enhanced hydrophilicity imparted by Ru-bound PTA ligand.

Molecular Modeling

Molecular docking of [**RuLCl]** and [**RuLPTA]** was performed using Autodock-Vina with the crystal structure of human serum transferrin proteins (hTf), PDB IDs: 2HAV and 3QYT, which are apo- and holoprotein, respectively.[S1] For docking, 2HAV was aligned against 3QYT. Both the protein structures were initialized for docking by removing the water molecules or any other non-protein moieties present in the crystal structure. The 2HAV and 3QYT were protonated based on physiological pH value *i.e.* pH=7.2. AutoDockTool (ADT) was used to merge the non-polar hydrogen atoms into their parent heavy-atoms and the system was neutralized using Gasteiger charges.[S2] The crystal structure of [**RuLCl]** and [**RuLPTA**] was initially optimized at the PM6 level of theory, using the MOPAC program.[S3] The atoms corresponding to aromatic rings in the ligand molecules, as well as atoms bonded with Ru atom, were fixed during docking procedure while aliphatic chains in the ligand were allowed to rotate providing a wide range of conformational flexibility.

References

1. O. Trott and A. J. Olson, *J. Comput. Chem.,* 2010, **31**, 455-461.
2. G. M. Morris, R. Huey, W. Lindstrom, M. F. Sanner, R. K. Belew, D. S. Goodsell, A. J. Olson, *J. Computational Chemistry*, 2009, **16**, 2785-2791.
3. MOPAC2016, Version: 16.060W, Stewart, J. J. P. *Stewart Computational Chemistry*. Available online: http://OpenMOPAC.net.

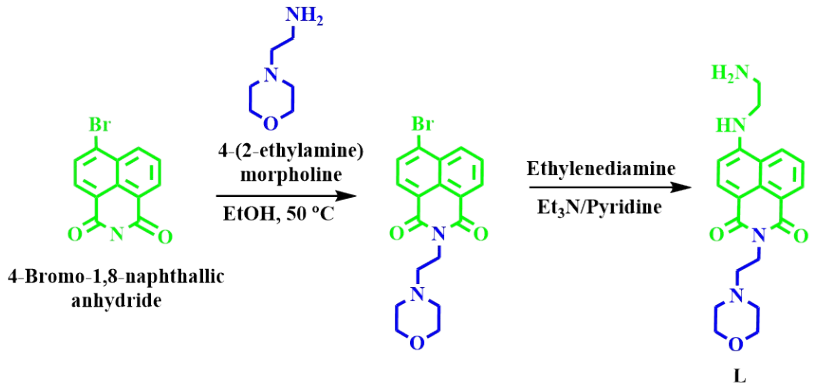

Scheme S1. Synthetic scheme for the preparation of the ligand L.

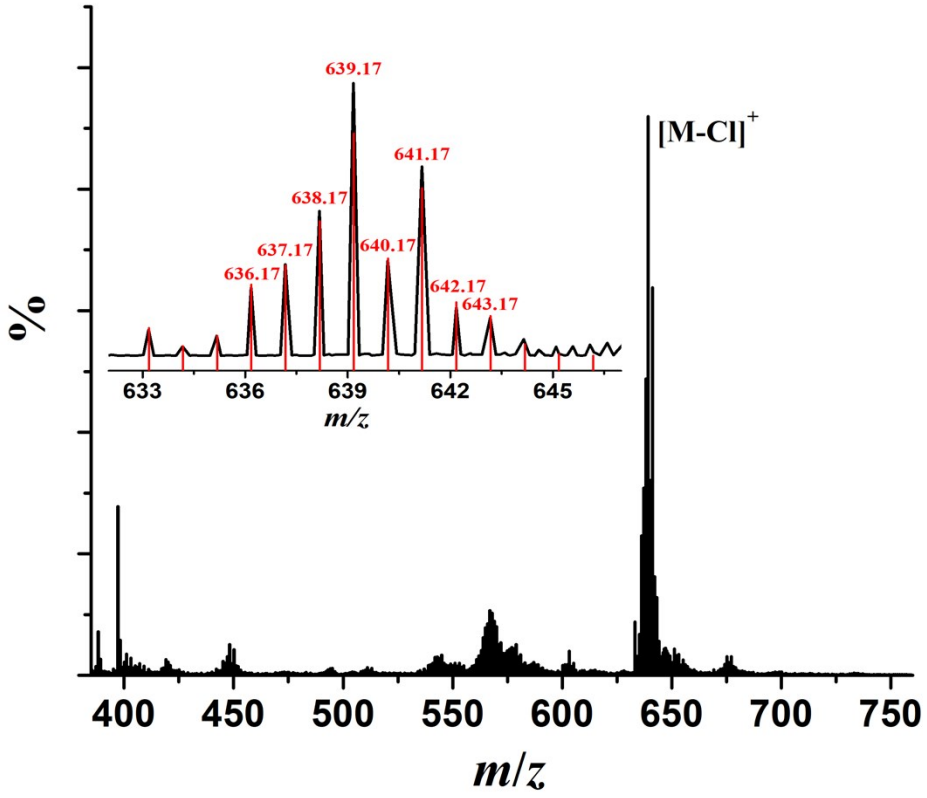

Figure S1. ESI-MS of the complex [**RuLCl**] in CH_2Cl_2. Inset shows *m/z* ($[M\text{-}Cl]^+$) calc. for $[C_{30}H_{38}N_4O_3ClRu]^+$: 639.17 (experimentally and theoretically) with matching isotopic distribution pattern.

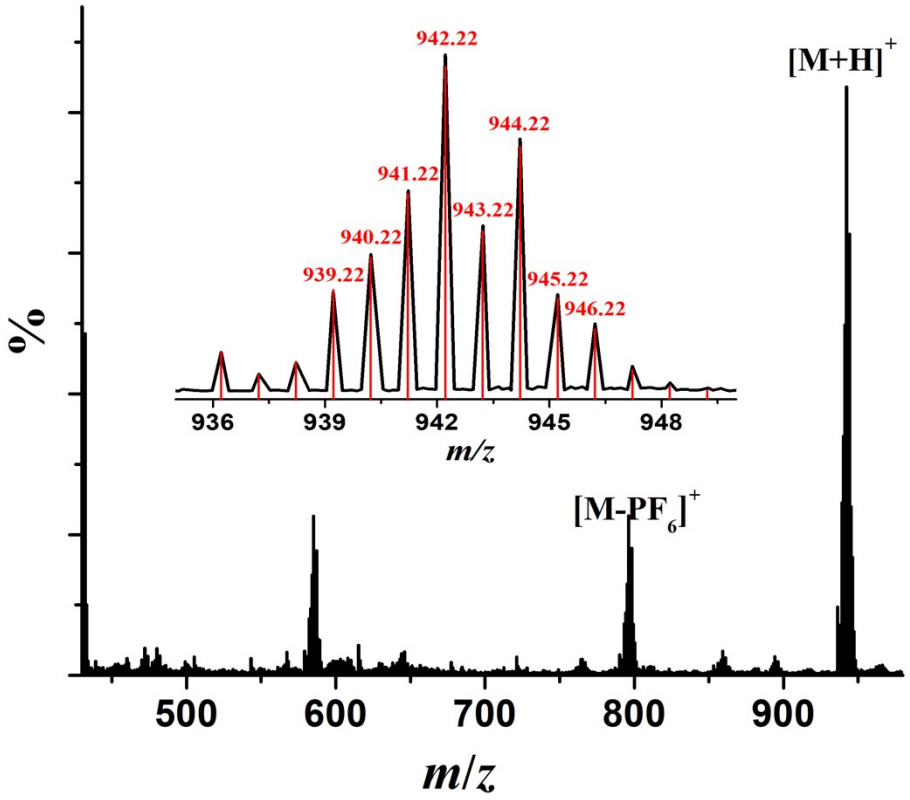

Figure S2. ESI-MS of the complex **[RuLPTA]** in CH_2Cl_2. Inset shows *m/z* ($[M+H]^+$) calc. for $[C_{36}H_{51}N_7O_3ClP_2F_6Ru]^+$: 942.22 (experimentally and theoretically) with matching isotopic distribution pattern.

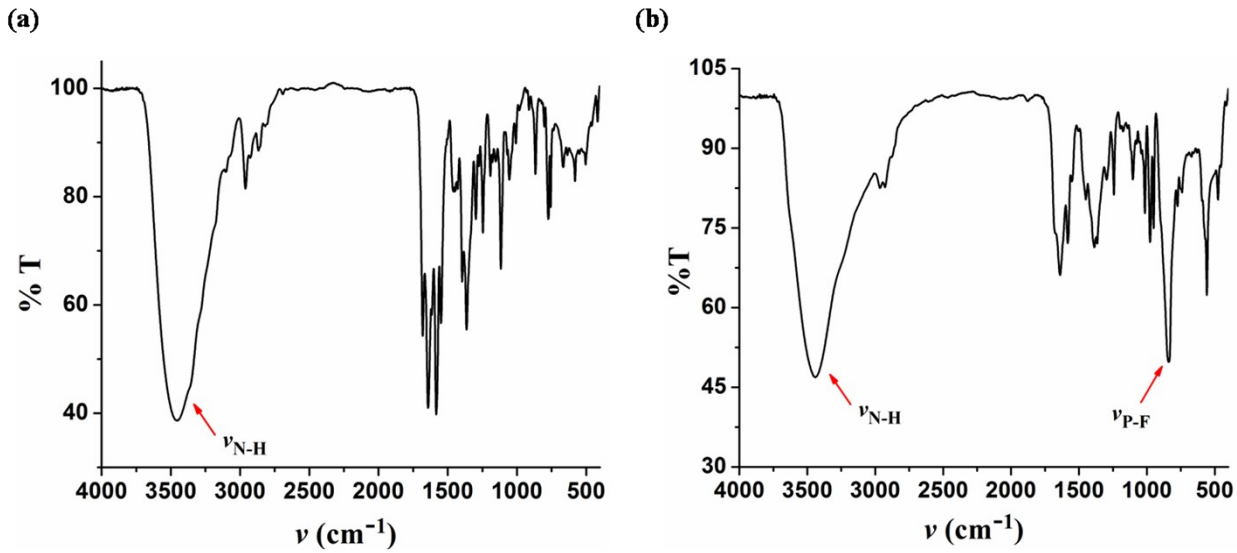

Figure S3. FTIR spectra of the complex (a) **[RuLCl]** and (b) **[RuLPTA]** in KBr phase, characteristic stretching frequencies were mentioned in the spectra.

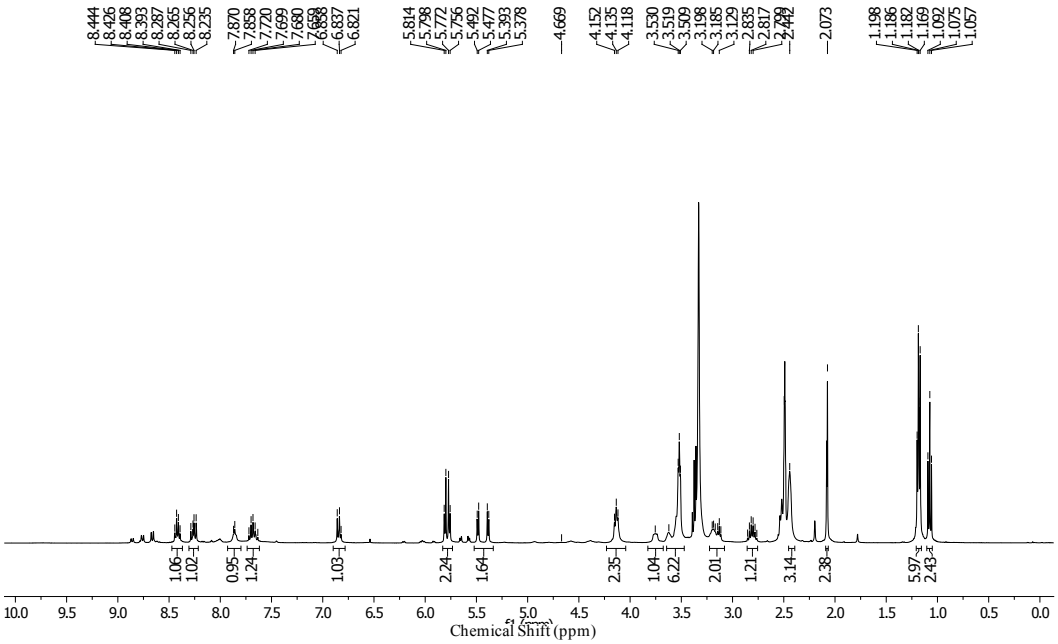

Figure S4. ^{1}H NMR spectra of [**RuLCl**] in DMSO-d_6 at 298 K (400 MHz) using TMS as reference.

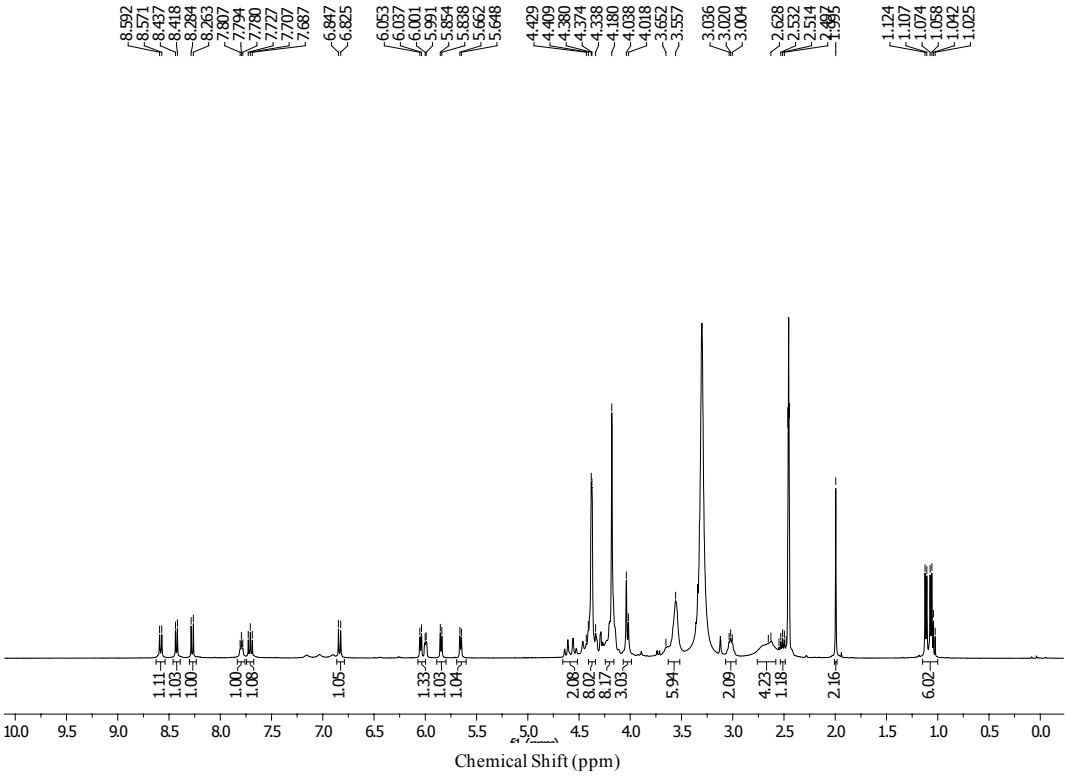

Figure S5 ^{1}H NMR spectra of [**RuLPTA**] in DMSO-d_6 at 298 K (400 MHz) using TMS as reference.

Table S1. Selected crystallographic data for the complex [**RuLCl**]

Parameters	[**RuLCl**]
Empirical formula	$C_{31}H_{40}Cl_4N_4O_3Ru$
Formula weight	759.54
Temperature/*K*	273.15
Crystal system	monoclinic
Space group	$P2_1/c$
a/Å	20.4731(12)
b/Å	19.8145(11)
c/Å	8.2261(5)
α/°	90
β/°	91.100(2)
γ/°	90
Volume/Å^3	3336.4(3)
Z	4
ρ_{calc}g/cm^3	1.512
μ/mm^{-1}	0.828
F(000)	1560.0
Crystal size/mm^3	0.2 × 0.16 × 0.12
Radiation	M_oK_α (λ = 0.71073)
2Θ range for data collection/°	5.688 to 56.534
Index ranges	-27 ≤ h ≤ 27, -26 ≤ k ≤ 26, -10 ≤ l ≤ 10
Reflections collected	52151
Independent reflections	8256 [R_{int} = 0.0479, R_{sigma} = 0.0313]
Data/restraints/parameters	8256/0/391
Goodness-of-fit on F^2	1.080
R_1[a] and wR_2[b] [[I>=2σ (I)]	0.0310, 0.0780
R_1 and wR_2 [all data]	0.0415, 0.0835
Largest diff. peak/hole / e Å^{-3}	0.47/-0.54

[a] $R_1=\Sigma||F_0|-|F_C||/\Sigma|F_0|$; [b] $wR_2=\{\Sigma[w(F_0^2-F_C^2)]/\Sigma[w(F_0^2)^2]\}^{1/2}$

Table S2. Selected bond lengths (Å) and angles (°) of the complex [**RuLCl**] with e.s.d.s. in parentheses.

[**RuLCl**]	Bond distance
Ru(1)-Cl(1)	2.4057(6)
Ru(1)-Cl(2)	2.4394(6)
Ru(1)-N(1)	2.1312(18)
Ru(1)-C(5)	2.194(2)
Ru(1)-C(3)	2.193(2)
Ru(1)-C(4)	2.165(2)
Ru(1)-C(6)	2.155(2)
Ru(1)-C(7)	2.173(2)
Ru(1)-C(2)	2.208(2)
[**RuLCl**]	Bond angles
Cl(2)-Ru(1)-Cl(1)	89.92(2)
N(1)-Ru(1)-Cl(1)	79.96(5)
N(1)-Ru(1)-Cl(2)	80.83(5)
N(1)-Ru(1)-C(5)	100.93(8)
N(1)-Ru(1)-C(3)	169.39(8)
N(1)-Ru(1)-C(4)	131.43(8)
N(1)-Ru(1)-C(6)	93.24(8)
N(1)-Ru(1)-C(7)	112.19(8)
N(1)-Ru(1)-C(2)	147.37(8)
C(5)-Ru(1)-Cl(1)	104.85(6)
C(5)-Ru(1)-Cl(2)	165.22(6)
C(5)-Ru(1)-C(2)	81.84(9)
C(3)-Ru(1)-Cl(1)	99.43(7)
C(3)-Ru(1)-Cl(2)	109.79(7)
C(3)-Ru(1)-C(5)	68.88(9)
C(3)-Ru(1)-C(2)	37.09(9)
C(4)-Ru(1)-Cl(1)	87.57(6)
C(4)-Ru(1)-Cl(2)	146.37(7)
C(4)-Ru(1)-C(5)	37.92(8)
C(4)-Ru(1)-C(3)	38.15(9)

C(4)-Ru(1)-C(7)	80.85(9)
C(4)-Ru(1)-C(2)	68.29(9)
C(6)-Ru(1)-Cl(1)	140.91(6)
C(6)-Ru(1)-Cl(2)	127.26(6)
C(6)-Ru(1)-C(5)	38.31(8)
C(6)-Ru(1)-C(3)	80.52(9)
C(6)-Ru(1)-C(4)	68.23(9)
C(6)-Ru(1)-C(7)	38.00(8)
C(6)-Ru(1)-C(2)	68.68(9)
C(7)-Ru(1)-Cl(1)	167.01(7)
C(7)-Ru(1)-Cl(2)	96.44(6)
C(7)-Ru(1)-C(5)	69.20(8)
C(7)-Ru(1)-C(3)	67.76(9)
C(7)-Ru(1)-C(2)	38.10(9)
C(2)-Ru(1)-Cl(1)	131.23(7)
C(2)-Ru(1)-Cl(2)	88.87(6)

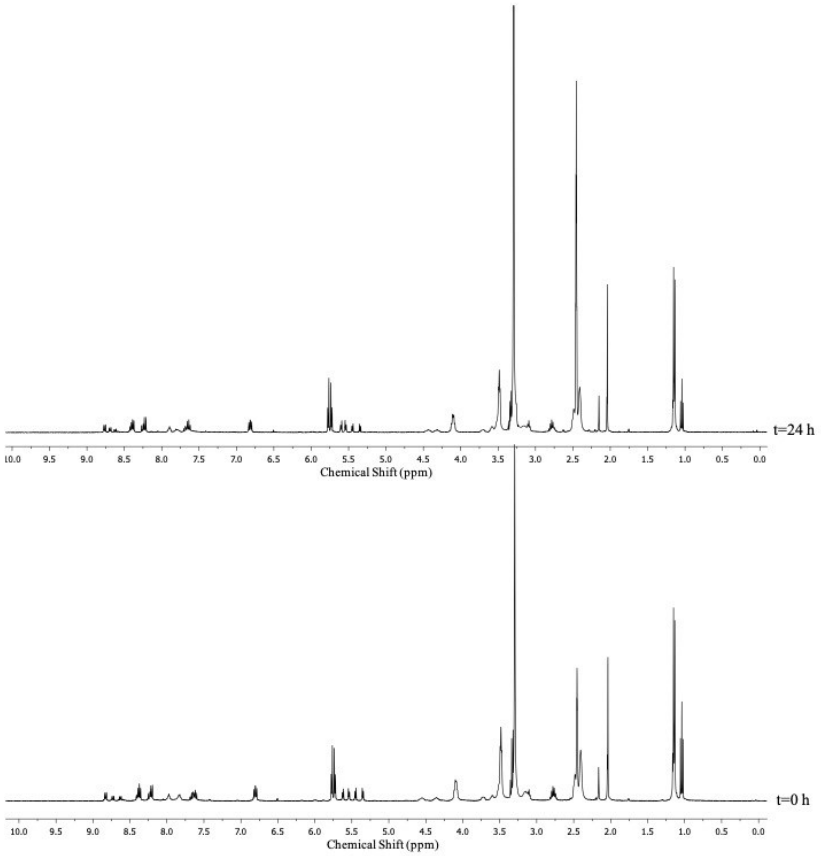

Figure S6. ^{1}H NMR spectra showing the stability of [**RuLCl**] in DMSO-d_6 over 24 h.

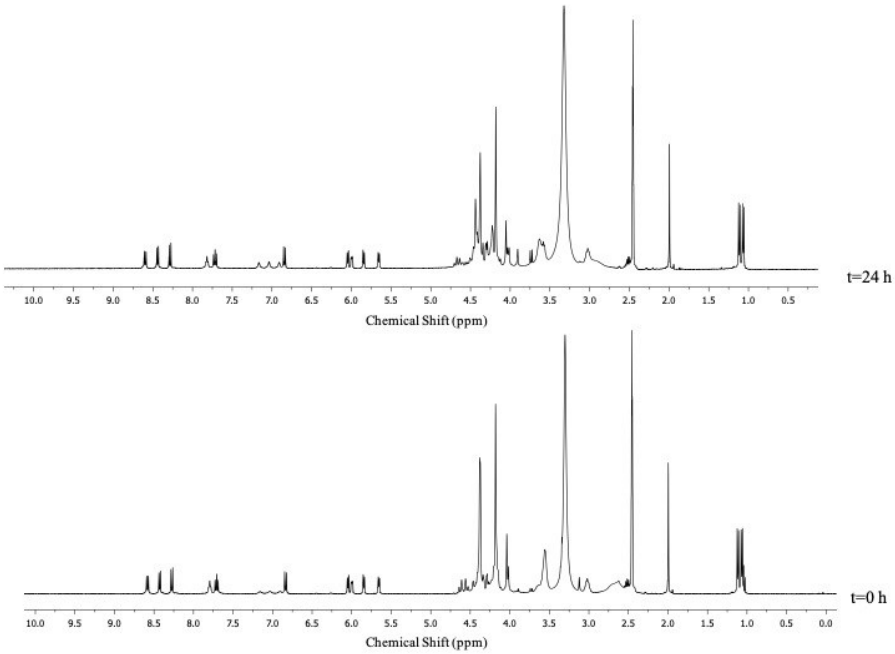

Figure S7. ^{1}H NMR spectra showing the stability of [**RuLPTA**] in DMSO-d_6 over 24 h.

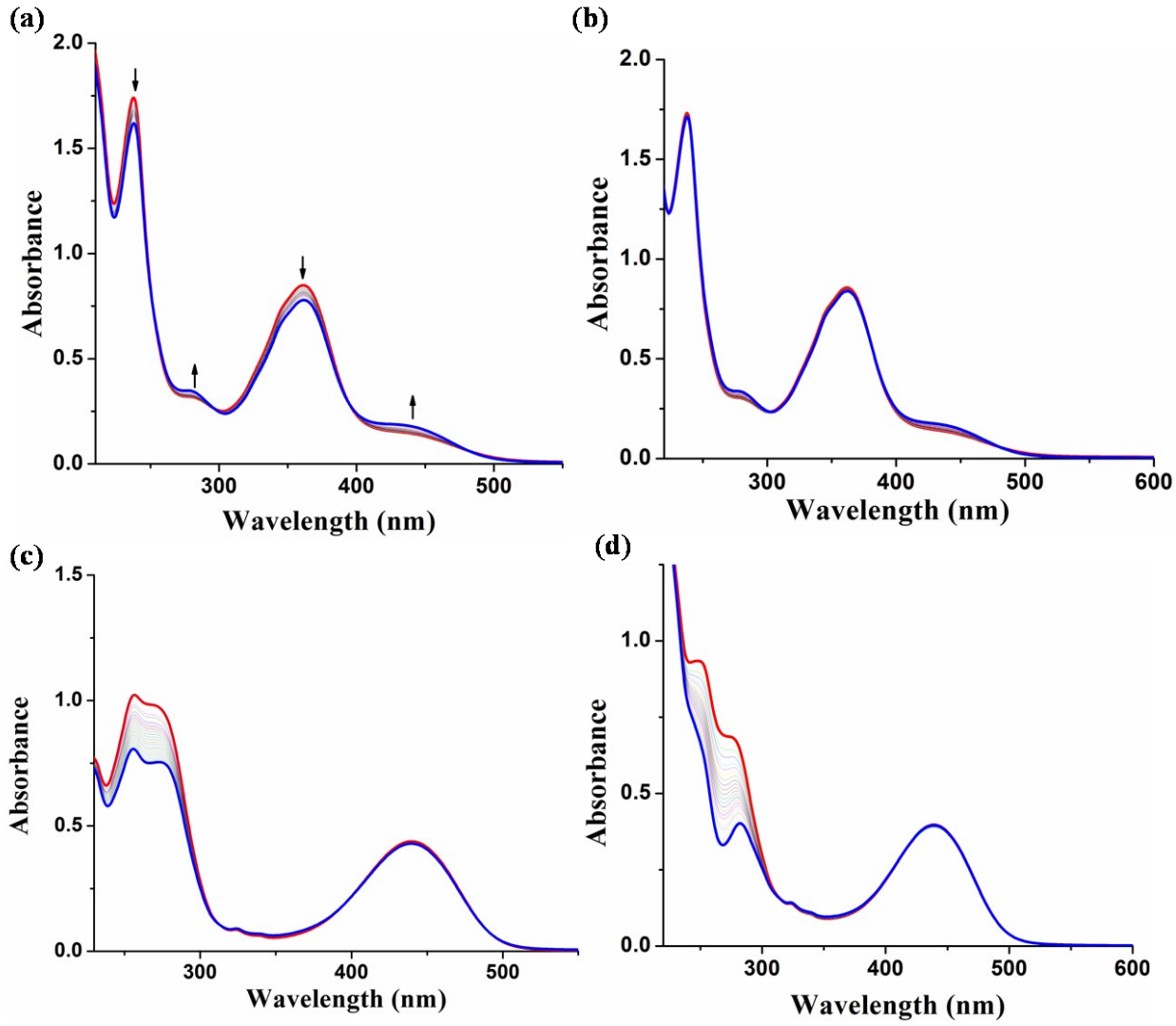

Figure S8. Time dependent absorption spectral changes of the complex [**RuLCl**] (54 μM) in (a) 4 mM NaCl-H_2O medium, (b) 100 mM NaCl-H_2O medium and [**RuLPTA**] (79 μM) in (c) 4 mM NaCl-H_2O medium, (d) 100 mM NaCl-H_2O medium for 2 h at 298 K.

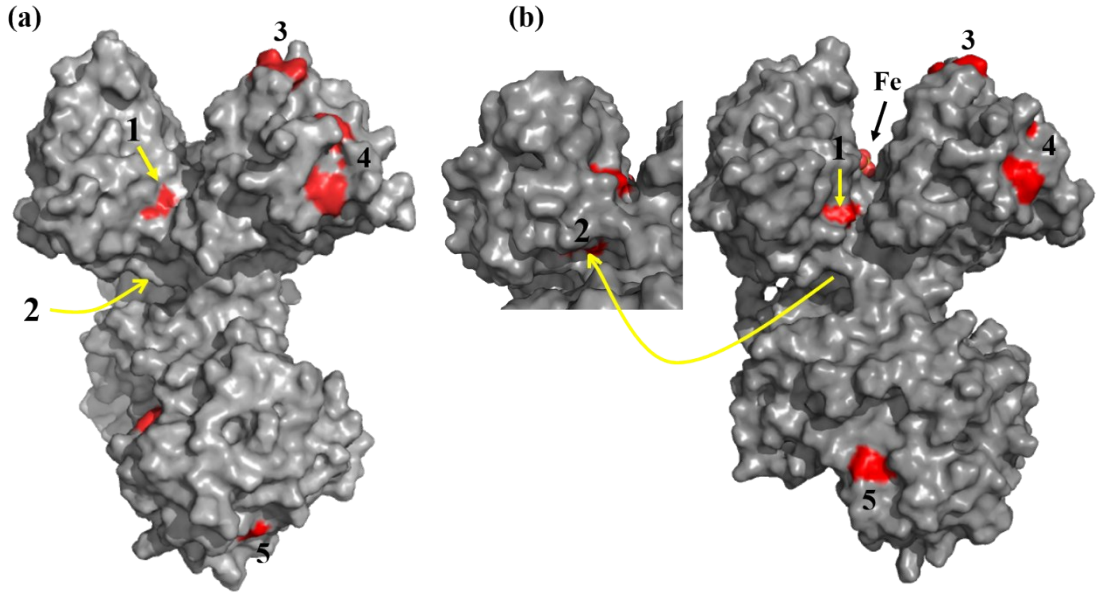

Figure S9. Five designated sites used for molecular docking shown on the vdW surface of **a)** apo-hTf (PDB code: 2HAV) and **b)** holo-hTf (PDB code: 3QYT). Each site contains histidine residue(s) (red), SITE1: HIS207; SITE2: HIS242; SITE3: HIS273 and HIS25 SITE4: HIS289 and HIS14; SITE5: HIS578 and HIS535. SITE2 *i.e.* site containing HIS242 lies in a cavity located under the N-lobe and is not visible in 2HAV while it is slightly exposed in 3QYT.

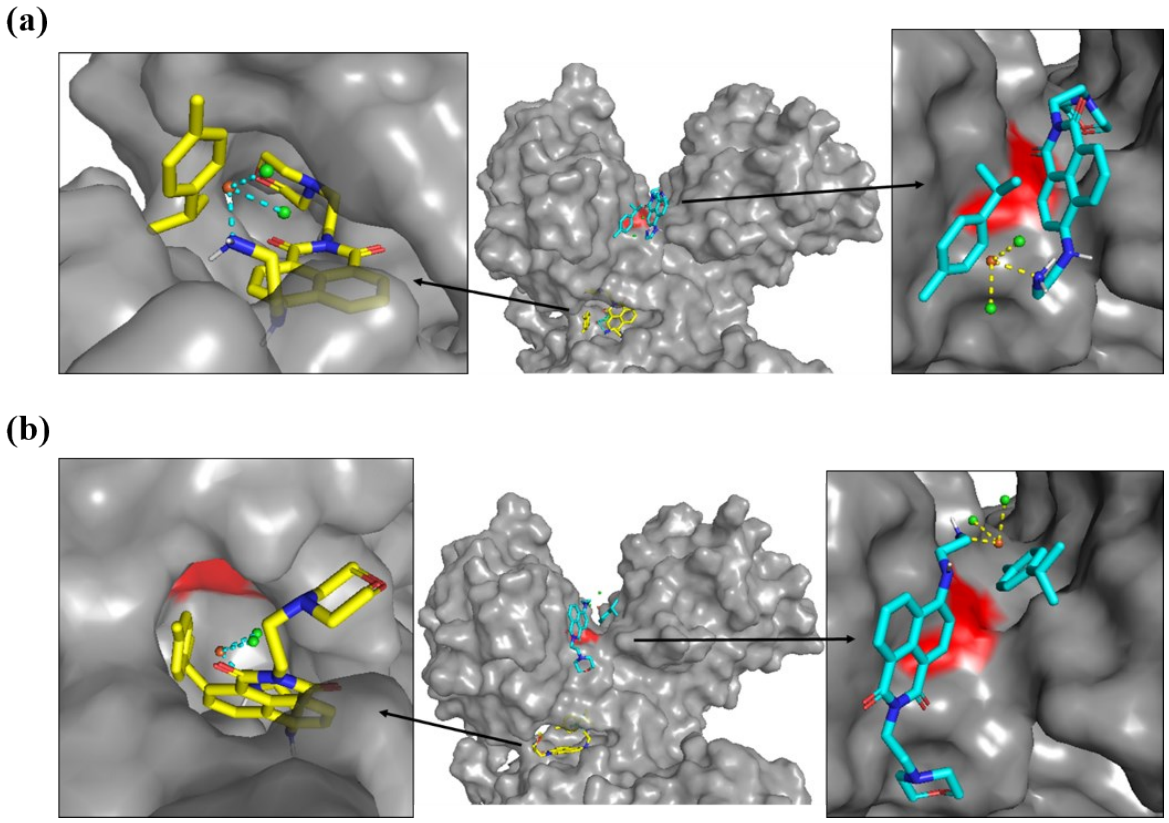

Figure S10. Conformation of [**RuLCl**] docked into the SITE1 and SITE2 on apo-hTf (PDB code: 2HAV) with a) highest binding affinity and b) third largest binding affinity. Latter is illustrated because Ru of [**RuLCl**] is closer to HIS207 at SITE1 and HIS242 at SITE2.

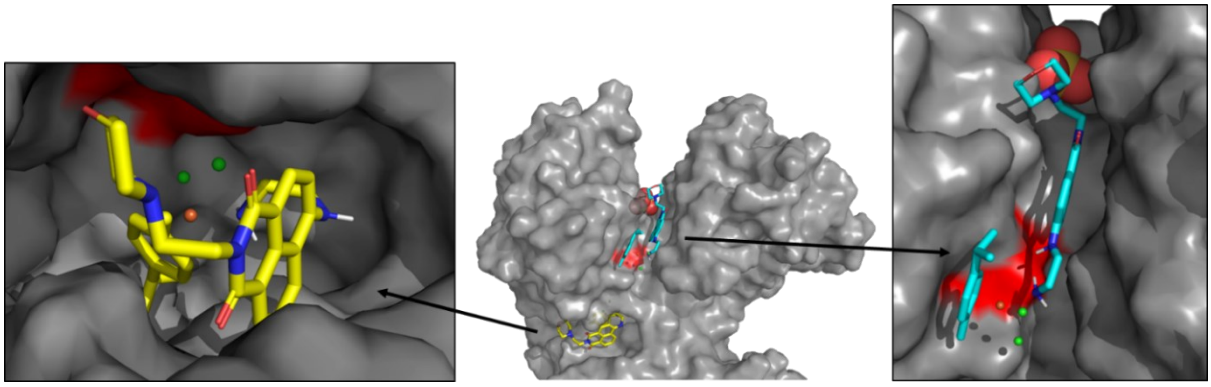

Figure S11. Conformation of [**RuLCl]** docked into the SITE1 and SITE2 on holo-hTf (PDB code: 3QYT) with largest binding affinity.

Table S3: Binding affinity of [**RuLCl**] at five different sites on apo-hTf (PDB code: 2HAV) and holo-hTf (PDB code: 3QYT) obtained using Autodock Vina.

	Binding Affinity (kcal/mol)									
Poses	**SITE1**		**SITE2**		**SITE3**		**SITE4**		**SITE5**	
	2HAV	**3QYT**	**2HAV**	**3QYT**	**2HAV**	**3QYT**	**2HAV**	**3QYT**	**2HAV**	**3QYT**
1	-7.0	-9.3	-7.5	-6.9	-5.2	-5.6	-5.1	-4.4	-5.4	-5.6
2	-6.9	-9.1	-7.3	-6.9	-4.8	-5.4	-4.9	-4.3	-5.1	-5.6
3	-6.7	-9.1	-7.2	-6.8	-4.7	-5.4	-4.8	-4.2	-4.9	-5.4
4	-6.7	-8.6	-7.0	-6.8	-4.6	-5.3	-4.8	-4.2	-4.8	-5.1
5	-6.7	-8.5	-7.0	-6.7	-4.4	-5.3	-4.7	-4.1	-4.7	-5.1
6	-6.7	-8.5	-6.9	-6.7	-4.4	-5.3	-4.7	-4.1	-4.7	-5.1
7	-6.6	-8.4	-6.8	-6.6	-4.3	-5.3	-4.7	-4.1	-4.6	-5.1
8	-6.6	-8.1	-6.7	-6.4	-4.3	-5.2	-4.6	-4.0	-4.6	-5.0
9	-6.5	-8.1	-6.7	-6.4	-4.3	-5.2	-4.6	-3.9	-4.4	-5.0

Table S4: Binding affinity of [**RuLPTA]** at five different sites on apo-hTf (PDB code: 2HAV) and holo-hTf (PDB code: 3QYT) obtained using Autodock Vina.

	Binding Affinity (kcal/mol)									
Poses	**SITE1**		**SITE2**		**SITE3**		**SITE4**		**SITE5**	
	2HAV	**3QYT**	**2HAV**	**3QYT**	**2HAV**	**3QYT**	**2HAV**	**3QYT**	**2HAV**	**3QYT**
1	-7.4	-9.1	-8.6	-8.7	-5.2	-5.4	-4.2	-4.8	-3.6	-6.2
2	-7.2	-9.0	-7.9	-8.6	-4.8	-5.0	-4.2	-4.7	-3.3	-6.0
3	-7.2	-8.8	-7.9	-8.5	-4.2	-4.9	-4.0	-4.7	-2.4	-6.0
4	-7.1	-8.2	-7.9	-8.4	-4.0	-4.7	-4.0	-4.6	-1.0	-5.9
5	-6.9	-8.2	-7.7	-8.3	-4.0	-4.6	-3.9	-4.6	--	-5.8
6	-6.9	-8.1	-7.4	-8.3	-3.5	-4.6	-3.8	-4.5	--	-5.8
7	-6.7	-7.9	-7.4	-8.2	-3.4	-4.5	-3.8	-4.5	--	-5.8
8	-6.7	-7.8	-7.2	-8.1	-3.3	-4.3	-3.6	-4.5	--	-5.8
9	-6.7	-7.8	-7.2	-7.8	-3.1	-4.3	-3.5	-4.5	--	-5.7

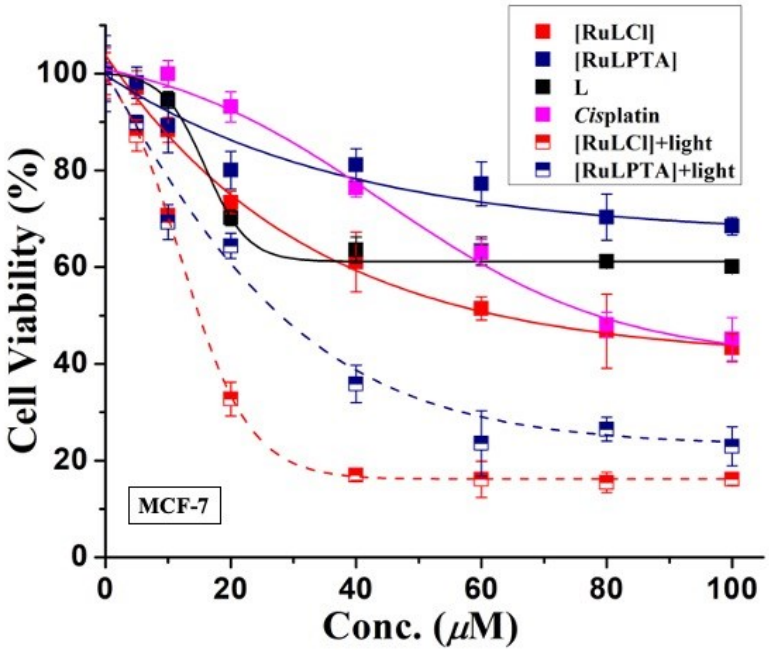

Figure S12. MTT assay plot for determination of IC_{50} values in MCF-7 cancer cells on incubation for 24 h of the complexes [**RuLCl**], [**RuLPTA**], L, *cis*platin (0-100 μM) in the dark and on light irradiation (λ_{irr}= 448 nm, 1030 mW @ 700mA from LuxeonStar LEDs) of the complexes for 1 h.

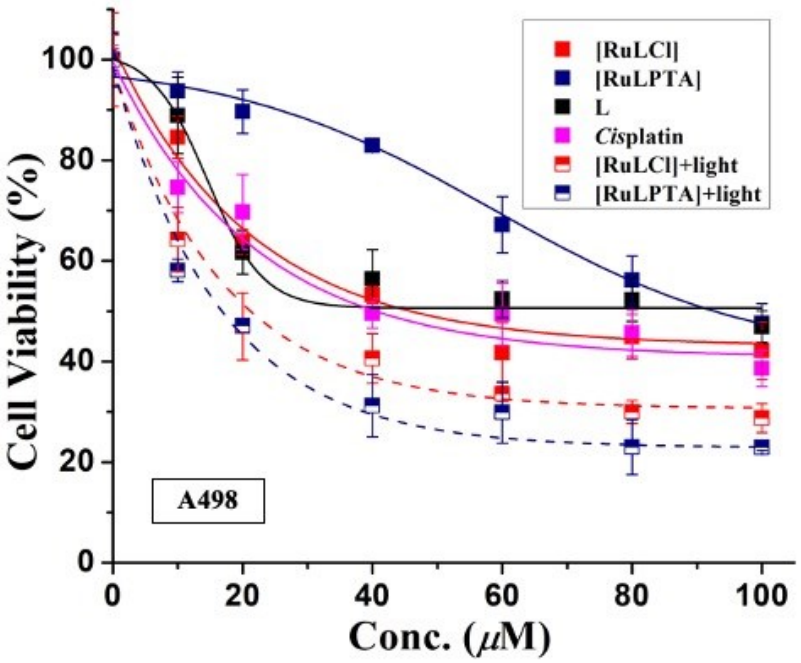

Figure S13. MTT assay plot for determination of IC_{50} values in A498 cancer cells on incubation for 24 h of the complexes [**RuLCl**], [**RuLPTA**], L, *cis*platin (0-100 μM) in the dark and on light irradiation (λ_{irr}= 448 nm, 1030 mW @ 700mA from LuxeonStar LEDs) of the complexes for 1 h.

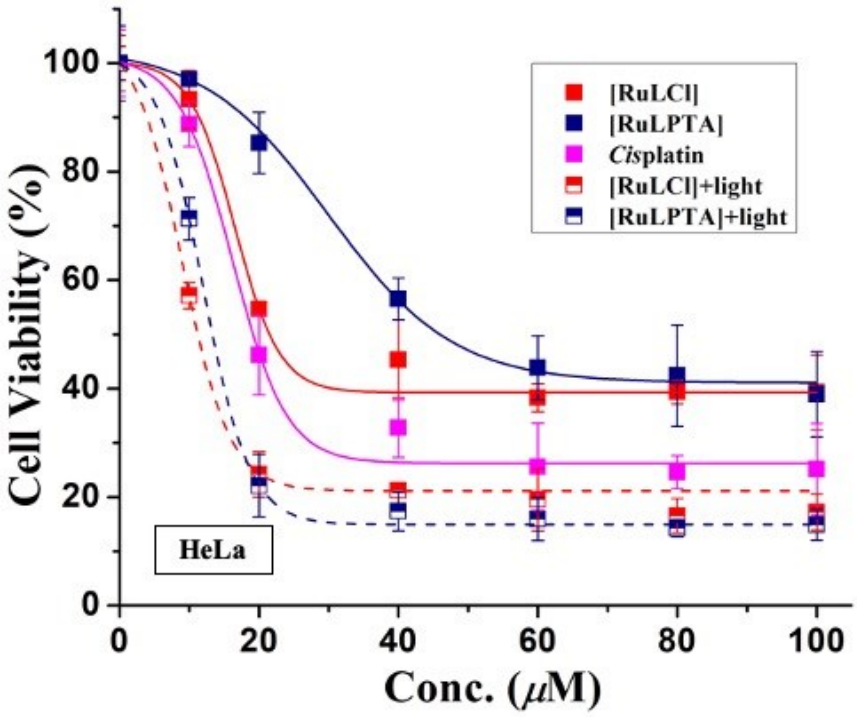

Figure S14. MTT assay plot for determination of IC_{50} values in HeLa cancer cells on incubation for 24 h of the complexes [**RuLCl**], [**RuLPTA**], *cis*platin (0-100 μM) in the dark and on light irradiation (λ_{irr}= 448 nm, 1030 mW @ 700mA from LuxeonStar LEDs) of the complexes for 1 h.

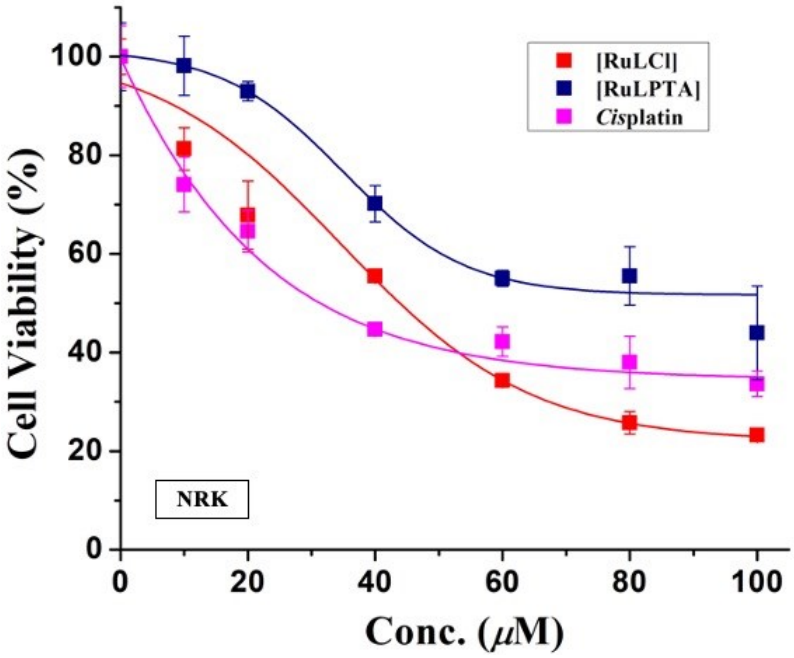

Figure S15. MTT assay plot for determination of IC_{50} values in NRK cells on incubation for 24 h of the complexes [**RuLCl**], [**RuLPTA**], and *cis*platin (0-100 μM) in the dark.

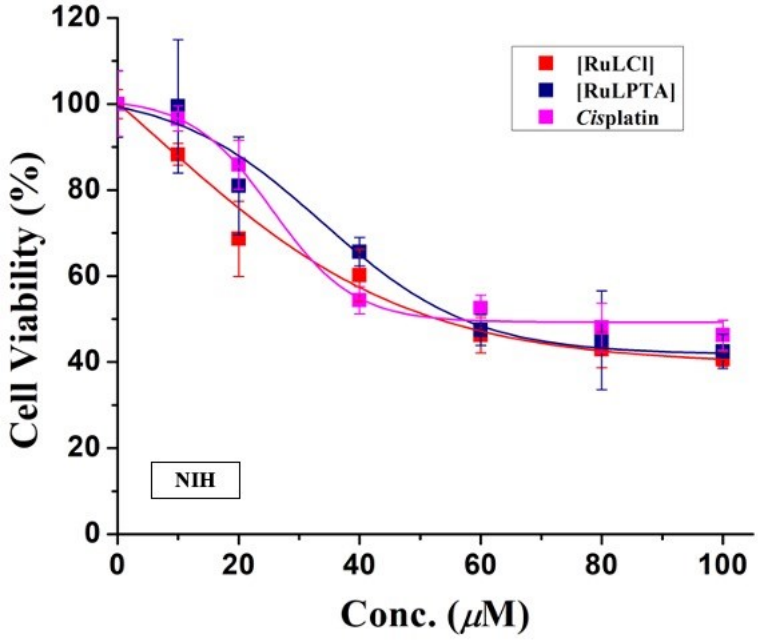

Figure S16. MTT assay plot for determination of IC_{50} values in NIH cells on incubation for 24 h of the complexes [**RuLCl**], [**RuLPTA**], and *cis*platin (0-100 μM) in the dark.